

1 The absorption coefficient of PbSe/CdSe core/shell colloidal quantum dots

2 Bram De Geyter^{1,2} and Zeger Hens^{2,a)}

3 ¹*Departement of Information Technology (INTEC), UGent, Sint-Pietersnieuwstraat 41,*
4 *B-9000 Gent, Belgium*

5 ²*Department of Inorganic and Physical Chemistry, UGent, Krijgslaan 281 (S3), B-9000 Gent, Belgium*

6 (Received 29 July 2010; accepted 21 September 2010; published online xx xx xxxx)

7 PbSe/CdSe core/shell colloidal quantum dots (QDs) are used as a model system to study the
8 absorption coefficient of colloidal QD heterostructures, consisting of at least two semiconductor
9 materials. We show that at energies far above the band gap (3.1 and 3.5 eV) the experimental
10 intrinsic absorption coefficient is in excellent agreement with the Maxwell–Garnett effective
11 medium theory for core/shell heterostructures and bulk values for the dielectric function. This
12 allows for a straightforward measurement of the QD concentration from the absorbance spectrum.
13 It also implies that basic optical measurements on core/shell heterostructures, such as measurements
14 of the oscillator strength and photoluminescence lifetime, can be corrected for the local field
15 reduction in QD heterostructures. © 2010 American Institute of Physics. [doi:10.1063/1.3499754]

17 Colloidal quantum dot (QD) research is driven by the
18 combination of tunable electronic and optical properties, de-
19 pending on the size and shape of the QDs, and an easy,
20 solution-based fabrication and processing. While QDs con-
21 sisting of a single semiconductor with an organic ligand cap-
22 ping, show promising properties for applications in lasers,
23 detectors, and solar cells,¹ their drawbacks, such as oxidation
24 and fast Auger recombination, shifted the focus of the re-
25 search field to QD heterostructures, combining at least two
26 semiconductors in a core/shell nanocrystal.

27 Since colloidal QDs are made in a wet chemical synthe-
28 sis, the basic characterization is mostly done on QDs sus-
29 pended in an organic solvent. Because of their small size, the
30 macroscopic optical properties of suspended QDs are deter-
31 mined both by the intrinsic optical properties and by the
32 surrounding medium. This effect is typically described by the
33 Maxwell–Garnett effective medium theory. The importance
34 of this effect can hardly be underestimated, as it will alter the
35 absorbance, the photoluminescence (PL) peak position and
36 emission rate and the PL quantum yield,² depending on the
37 surrounding medium or solvent. For example, Moreels *et al.*³
38 used this theory to calculate the dielectric function of PbSe,
39 PbS, and PbTe colloidal QDs and study the effect of quantum
40 confinement on these elementary material properties. This
41 effect is typically described by the local field factor f_{LF} ,
42 which is the ratio of the field inside the QD and the field in
43 the surrounding medium.

44 Here, we analyze the effect of the effective medium on
45 the absorbance (A) of core/shell PbSe/CdSe QDs, where not
46 only the solvent but also the inorganic core/shell structure
47 determines the local field factor. To quantify the spectrum of
48 the absorbance (A), it is converted to the spectrum of the
49 intrinsic absorption coefficient μ_i . For this, the QD volume
50 fraction f and the cuvette length L are needed as follows:

$$51 \mu_i = \frac{\ln 10 \times A}{fL}. \quad (1)$$

52 The intrinsic absorption coefficient μ_i provides the charac-
53 teristic decay length of the light intensity in a hypothetical
54 medium with a QD volume fraction of one.

For PbSe,⁴ PbS,⁵ wurtzite and zinc blende CdSe,^{6–8} 55
InAs,⁹ and ZnO¹⁰ QDs, it was shown that at high energies 56
(3.1 eV for PbSe and PbS, 3.54 eV for CdSe, 2.76 eV for 57
InAs, and 5.0 eV for ZnO), μ_i is independent of the QD size. 58
Moreover, it generally coincides with the theoretical value 59
calculated using bulk optical constants and the Maxwell– 60
Garnett effective medium theory as follows:^{11,12} 61

$$62 \mu_i = \frac{2\pi}{\lambda n_s} \text{Im}(\epsilon_c) |f_{LF}|^2. \quad (2)$$

Here, n_s is the solvent refractive index, ϵ_c and ϵ_s the complex 63
dielectric function of the QD material and the solvent, re- 64
spectively, and λ the wavelength. For spherical particles, the 65
local field factor reads as follows: 66

$$67 f_{LF} = \frac{3\epsilon_s}{\epsilon_c + 2\epsilon_s}. \quad (3)$$

The fact, that at short wavelengths a bulklike absorption 68
coefficient is found, means that the electronic states at high 69
energies are not quantum confined but form a continuum in 70
these QDs. Hence the QD concentration [QD], an essential 71
quantity to assess synthesis quality and to control deposition, 72
can be determined as follows from the absorbance at high 73
energies, irrespective of size dispersion, using the Beer– 74
Lambert law and μ_i as calculated above: 75

$$76 [\text{QD}] = \frac{A}{\epsilon L} = \frac{A \ln 10}{\mu_i N_A V_{\text{QD}} L}. \quad (4)$$

Here N_A is Avogadro's constant and V_{QD} the volume of the 77
QD. 78

For core/shell QDs, the formulas above cannot be ap- 79
plied directly, since the shell will alter the dielectric screen- 80
ing. An expression for the absorption coefficient of core/shell 81
particles was proposed by Neeves *et al.*^{13,14} If the volume 82
fraction of core/shell particles in solution is small, it reads as 83
follows: 84

$$85 \mu_i = \frac{2\pi}{\lambda n_s} \text{Im}(3\epsilon_s \beta),$$

^{a)}Electronic mail: zeger.hens@ugent.be.

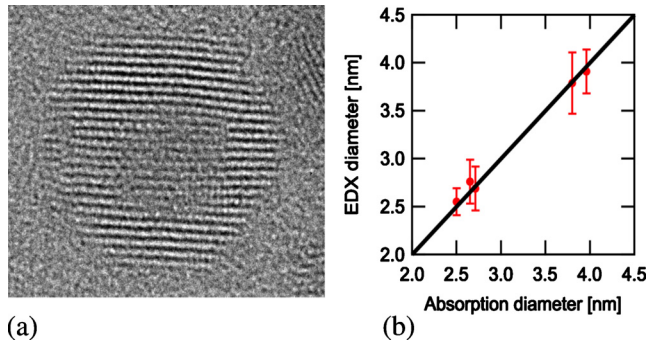


FIG. 1. (Color online) (a) HR-TEM image of a PbSe/CdSe core/shell QD, clearly showing the PbSe core and the CdSe shell. (b) Diameter determined from EDX vs diameter determined from the position of the first absorption peak, using the PbSe sizing curve. The black line indicates a 1-to-1 relationship (Ref. 4).

$$86 \quad \text{with } \beta = \left(\frac{\epsilon_{sh}\epsilon_a - \epsilon_s\epsilon_b}{\epsilon_{sh}\epsilon_a + 2\epsilon_s\epsilon_b} \right),$$

$$87 \quad \epsilon_a = \epsilon_c \left(3 - 2 \frac{V_{sh}}{V_{QD}} \right) + 2\epsilon_{sh} \frac{V_{sh}}{V_{QD}},$$

$$88 \quad \epsilon_b = \epsilon_c \frac{V_{sh}}{V_{QD}} + \epsilon_{sh} \left(3 - \frac{V_{sh}}{V_{QD}} \right). \quad (5)$$

89 Here, ϵ_{sh} denotes the complex dielectric function of the shell.
 90 Importantly, μ_i becomes dependent on the ratio between the
 91 shell and the total QD volume for core/shell heterostructures.
 92 This is purely an effect of the change in the effective medium
 93 and not an effect of quantum confinement. Hence, to com-
 94 pare theory with experiment, a precise knowledge of the core
 95 diameter and shell thickness is essential for QD heterostruc-
 96 tures.

97 We take the example of PbSe/CdSe QDs, made by cation
 98 exchange on PbSe QDs,¹⁵ to study the absorption coefficient
 99 of QD heterostructures. They offer an ideal test case, since
 100 the total QD diameter and the concentration remains constant
 101 throughout the exchange procedure. Indeed, as Pb atoms in
 102 the PbSe lattice are gradually replaced by Cd atoms, a CdSe
 103 shell with increasing thickness is formed for prolonged ex-
 104 change times. This is confirmed by high-resolution transmis-
 105 sion electron microscope (HR-TEM) images [see Fig. 1(a)],
 106 which clearly show the CdSe shell around the PbSe core.
 107 HR-TEM however is not suitable for high-throughput mea-
 108 surements of the core diameter and shell thickness. Hence we

use TEM-based energy dispersive x-ray spectroscopy (EDX) **109**
 to determine the Pb/Se ratio of the original PbSe QDs and of **110**
 the derived PbSe/CdSe QDs. Since the Se-content remains **111**
 constant throughout the exchange process, we can calculate **112**
 the PbSe core diameter from the reduction in the Pb/Se ratio **113**
 and the parent PbSe QD diameter. These values are in good **114**
 agreement with the core diameters obtained using the loca- **115**
 tion of the first absorption peak and the PbSe QD sizing **116**
 curve⁴ [see Fig. 1(b)]. Recent work by Zhang *et al.*¹⁶ using a **117**
 similar approach for the CdSe growth confirm this result. **118**
 They observe a shift of only 32 nm in the absorption spectra **119**
 upon growth of three CdSe monolayers (~ 1 nm shell thick- **120**
 ness), which corresponds to a shift in the diameter of just **121**
 0.17 nm, less than a Cd or Se monolayer. This illustrates that **122**
 we can use the PbSe QD sizing curve to determine the core **123**
 diameter and shell thickness of PbSe/CdSe QDs, provided **124**
 that the parent PbSe QD diameter is known. **125**

Under the assumption that the initial, known QD volume **126**
 fraction does not change during the cation exchange process, **127**
 the spectrum of μ_i [see Fig. 2(a)] is readily obtained from the **128**
 absorption spectrum of a PbSe/CdSe suspension [see Eq. **129**
 (1)]. In Fig. 2(a), spectra for several differently sized PbSe **130**
 QDs clearly coincide at energies far above the band gap, **131**
 whereas the spectra for PbSe/CdSe QDs show a broad band **132**
 of values due to the influence of the CdSe shell. Figure 2(c) **133**
 shows a set of experimentally determined intrinsic absorp- **134**
 tion coefficients at 3.1 eV ($\mu_{3.1 \text{ eV}}$) and 3.5 eV ($\mu_{3.5 \text{ eV}}$) for **135**
 PbSe/CdSe QDs with different total diameter, core diameter **136**
 and shell thickness as a function of the shell/QD volume **137**
 ratio V_{sh}/V_{QD} . For small shells μ_i slightly increases, reaching **138**
 a maximum value. For larger shells, μ_i decreases rapidly. **139**
 The full lines represent $\mu_{i,th}$ values calculated with bulk **140**
 PbSe and CdSe optical constants at 3.1 eV (400 nm) and 3.5 **141**
 eV (355 nm).^{17,18} Clearly, we find an excellent agreement **142**
 between these theoretical values and the experimental results **143**
 for $\mu_{3.1 \text{ eV}}$ and $\mu_{3.5 \text{ eV}}$ [see Fig. 2(c)]. **144**

Following Neeves *et al.*,¹³ the local field factor in the **145**
 core of a core/shell QD reads as follows: **146**

$$f_{LF} = \frac{9\epsilon_{sh}\epsilon_s}{\epsilon_{sh}\epsilon_a + 2\epsilon_s\epsilon_b}. \quad (6) \quad 147$$

At 3.1 eV, $|f_{LF}|^2$ gradually increases from the value of PbSe **148**
 core QDs to that of CdSe core QDs, which accounts for the **149**
 initial rise of the intrinsic absorption coefficient of PbSe/**150**
 CdSe core/shell QDs for small shells [see Fig. 2(b)]. With **151**
 thicker shells, μ_i decreases, because the contribution of the **152**
 CdSe shell, which absorbs less than the PbSe core, becomes **153**

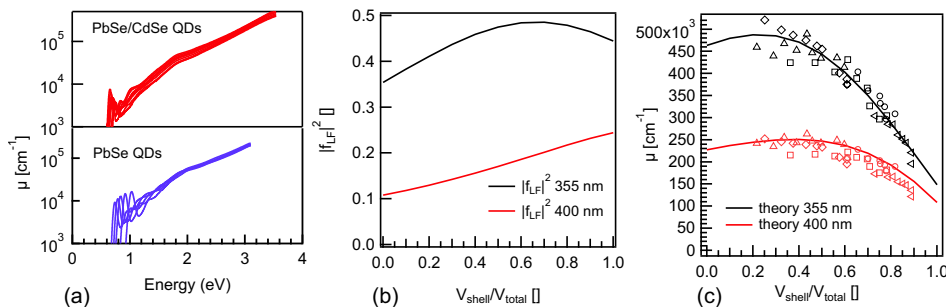


FIG. 2. (Color online) (a) Spectra of μ_i for PbSe/CdSe QDs with constant V_{QD} and increasing V_{sh} and PbSe QDs with varying diameters. (b) Local field factor calculated for PbSe/CdSe core/shell QDs at 355 nm and 400 nm. In the limiting case it becomes the local field factor for PbSe QDs ($V_{sh}=0$) or CdSe QDs ($V_{sh}=V_{total}$). (c) Intrinsic absorption coefficient $\mu_{3.5 \text{ eV}}$ at 355 nm and $\mu_{3.1 \text{ eV}}$ at 400 nm for PbSe/CdSe core/shell QDs as predicted by theory (line) and as measured (with total diameter of circles=5.2 nm, squares=5.8 nm, triangles=7.8 nm, left arrows=4.5 nm, and diamonds=7.5 nm).

154 more important. The great correspondence between the ex-
 155 perimental and theoretical values for μ_i proves that the
 156 Maxwell–Garnett effective medium theory can adequately
 157 describe the absorption of QD heterostructures at high ener-
 158 gies. At these energies, the energy levels of both the PbSe
 159 core and the CdSe shell form a continuum, allowing us to
 160 treat the absorption of these QD heterostructures using bulk
 161 values.

162 Calculating μ_i using the Maxwell–Garnett effective me-
 163 dium theory and bulk values for the dielectric function offers
 164 an elegant and reliable way to determine the QD concentra-
 165 tion of suspensions of QD heterostructures [see Eq. (4)],
 166 based on a straightforward absorbance measurement and
 167 knowledge of the core and shell size. This is essential for the
 168 successful integration of these QDs in applications such as
 169 light-emitting diodes and lasers. In typical synthesis schemes
 170 for core/shell growth, where the concentration remains con-
 171 stant, it also allows for direct monitoring of the dynamics of
 172 shell growth. For studies on the intrinsic carrier dynamics in
 173 QD heterostructures, the contribution of the change in the
 174 local field can be taken into account, using this effective
 175 medium theory.

176 In summary, we used PbSe/CdSe QDs as a model system
 177 to test the validity of the Maxwell–Garnett model for colloi-
 178 dal core/shell QDs. These QDs have a well-defined concen-
 179 tric core/shell structure and both size and concentration can
 180 be determined easily. We have shown that their intrinsic ab-
 181 sorption coefficient at energies well above the band edge can
 182 be predicted using the Maxwell–Garnett effective medium
 183 theory and bulk values for the dielectric function. The valid-
 184 ity of this model has important implications for colloidal QD
 185 heterostructure research, since the local field influences all
 186 optical characterization methods. It changes, for example,
 187 the magnitude of the absorption spectrum and the PL decay
 188 rate. Hence this model not only offers an easy way to deter-
 189 mine concentrations of QD suspensions but has to be taken

into account when extracting the intrinsic physics of colloi- 190
 dal QD heterostructures from standard optical measurements. 191

This project is funded by the Bijzonder Onderzoeks- 192
 fonds (BOF-UGent), the Belgian Science Policy Office 193
 (Grant No. IAP P6/10), and the EU Seventh Framework Pro- 194
 gram (EU-FP7 ITN Herodot under Grant No. 214954). 195

- ¹E. H. Sargent, *Adv. Mater. (Weinheim, Ger.)* **17**, 515 (2005). 196
- ²A. Kigel, M. Brumer, G. I. Maikov, A. Sashchiuk, and E. Lifshitz, *Small* **5**, 1675 (2009). 197
- ³I. Moreels, G. Allan, B. De Geyter, L. Wirtz, C. Delerue, and Z. Hens, *Phys. Rev. B* **81**, 235319 (2010). 199
- ⁴I. Moreels, K. Lambert, D. De Muynck, F. Vanhaecke, D. Poelman, J. C. Martins, G. Allan, and Z. Hens, *Chem. Mater.* **19**, 6101 (2007). 201
- ⁵I. Moreels, K. Lambert, D. Smeets, D. De Muynck, T. Nollet, J. C. Martins, F. Vanhaecke, A. Vantomme, C. Delerue, G. Allan, and Z. Hens, *ACS Nano* **3**, 3023 (2009). 203
- ⁶C. Leatherdale, W. Woo, F. Mikulec, and M. Bawendi, *J. Phys. Chem. B* **106**, 7619 (2002). 206
- ⁷J. Jasieniak, L. Smith, J. van Embden, and P. Mulvaney, *J. Phys. Chem. C* **113**, 19468 (2009). 208
- ⁸R. K. Čapek, I. Moreels, K. Lambert, D. De Muynck, Q. Zhao, A. Vantomme, F. Vanhaecke, and Z. Hens, *J. Phys. Chem. C* **114**, 6371 (2010). 211
- ⁹P. Yu, M. Beard, R. Ellingson, S. Ferrere, C. Curtis, J. Drexler, F. Luiszer, and A. Nozik, *J. Phys. Chem. B* **109**, 7084 (2005). 213
- ¹⁰P. Lommens, K. Lambert, F. Loncke, D. De Muynck, T. Balkan, F. Vanhaecke, H. Vrielinck, F. Callens, and Z. Hens, *ChemPhysChem* **9**, 484 (2008). 216
- ¹¹D. Ricard, M. Ghanassi, and M. Schanneklein, *Opt. Commun.* **108**, 311 (1994). 218
- ¹²A. Sihvola, *J. Electromagn. Waves Appl.* **15**, 715 (2001). 220
- ¹³A. Neeves and M. Birnboim, *J. Opt. Soc. Am. B* **6**, 787 (1989). 221
- ¹⁴A. Sihvola, *Electromagnetic Mixing Formulas and Applications* (IEE, London, UK, 1999), p. 295. 223
- ¹⁵J. Pietryga, D. Werder, D. Williams, J. Casson, R. Schaller, V. Klimov, and J. Hollingworth, *J. Am. Chem. Soc.* **130**, 4879 (2008). 225
- ¹⁶Y. Zhang, Q. Dai, X. Li, Q. Cui, Z. Gu, B. Zou, Y. Wang, and W. W. Yu, *Nanoscale Res. Lett.* **5**, 1279 (2010). 226
- ¹⁷N. Suzuki, K. Sawai, and S. Adachi, *J. Appl. Phys.* **77**, 1249 (1995). 228
- ¹⁸S. Ninomiya and S. Adachi, *J. Appl. Phys.* **78**, 4681 (1995). 229